

# Longitudinal EAS-Development Studies in the Air-Shower Experiment KASCADE-Grande

P. Doll<sup>b\*</sup>, W.D. Apel<sup>b</sup>, J.C. Arteaga-Velázquez<sup>a,†</sup>, K.Bekk<sup>b</sup>, M. Bertaina<sup>c</sup>, J. Blümer<sup>a,b</sup>, H. Bozdog<sup>b</sup>, I.M. Brancus<sup>d</sup>, P. Buchholz<sup>e</sup>, E. Cantoni<sup>c</sup>, A. Chiavassa<sup>c</sup>, F. Cossavella<sup>a,2</sup>, K. Daumiller<sup>b</sup>, V. de Souza<sup>a,3</sup>, F. di Pierro<sup>c</sup>, R. Engel<sup>b</sup>, J. Engler<sup>b</sup>, M. Finger<sup>a</sup>, D. Fuhrmann<sup>f</sup>, P.L. Ghia<sup>g</sup>, H.J. Gils<sup>b</sup>, R. Glasstetter<sup>f</sup>, C. Grupen<sup>e</sup>, A. Haungs<sup>b</sup>, D. Heck<sup>b</sup>, J.R. Hörandel<sup>a,4</sup>, T. Huege<sup>b</sup>, P.G. Isar<sup>b,5</sup>, K.-H. Kampert<sup>f</sup>, D. Kang<sup>a</sup>, D. Kickelbick<sup>e</sup>, H.O. Klages<sup>b</sup>, K. Link<sup>a</sup>, P. Łuczak<sup>h</sup>, M. Ludwig<sup>a</sup>, H.J. Mathes<sup>b</sup>, H.J. Mayer<sup>b</sup>, M. Melissas<sup>a</sup>, J. Milke<sup>b</sup>, B. Mitrica<sup>d</sup>, C. Morello<sup>g</sup>, G. Navarra<sup>c,6</sup>, S. Nehls<sup>b</sup>, J. Oehlschläger<sup>b</sup>, S. Ostapchenko<sup>b,7</sup>, S. Over<sup>e</sup>, N. Palmieria<sup>a</sup>, M. Petcu<sup>d</sup>, T. Pierog<sup>b</sup>, H. Rebel<sup>b</sup>, M. Roth<sup>b</sup>, H. Schieler<sup>b</sup>, F.G. Schröder<sup>b</sup>, O. Sima<sup>i</sup>, G. Toma<sup>d</sup>, G.C. Trinchero<sup>g</sup>, H. Ulrich<sup>b</sup>, A. Weindl<sup>b</sup>, J. Wochele<sup>b</sup>, M. Wommer<sup>b</sup>, J. Zabierowski<sup>h</sup>

<sup>a</sup>Institut für Experimentelle Kernphysik, KIT - Campus Süd, 76021 Karlsruhe, Germany

<sup>b</sup>Institut für Kernphysik, KIT - Campus Nord, 76021 Karlsruhe, Germany

<sup>c</sup>Dipartimento di Fisica Generale dell'Università, 10125 Torino, Italy

<sup>d</sup>National Institute of Physics and Nuclear Engineering, 7690 Bucharest, Romania

<sup>e</sup>Fachbereich Physik, Universität Siegen, 57068 Siegen, Germany

<sup>f</sup>Fachbereich Physik, Universität Wuppertal, 42097 Wuppertal, Germany

<sup>g</sup>Istituto di Fisica dello Spazio Interplanetario, INAF, 10133 Torino, Italy

<sup>h</sup>Soltan Institute for Nuclear Studies, 90950 Lodz, Poland

<sup>i</sup>Department of Physics, University Bucharest, 76900 Bucharest, Romania

A large area (128m<sup>2</sup>) Muon Tracking Detector (MTD), located within the KASCADE experiment, has been built with the aim to identify muons ( $E_\mu > 0.8\text{GeV}$ ) and their directions in extensive air showers by track measurements under more than 18 r.l. shielding. The orientation of the muon track with respect to the shower axis is expressed in terms of the radial- and tangential angles. By means of triangulation the muon production height  $H_\mu$  is determined. By means of  $H_\mu$ , a transition from light to heavy cosmic ray primary particle with increasing shower energy  $E_o$  from 1-10 PeV is observed. Muon pseudorapidity distributions for the first interactions above 15km are studied and compared to Monte Carlo simulations.

## 1. Introduction

Muons have never been used up to now to reconstruct the hadron longitudinal development of EAS with sufficient accuracy, due to the difficulty of building large area ground-based muon telescopes [1]. Muons are produced mainly by the decay of charged pions and kaons in a wide energy range. They are not always produced directly on the shower axis. Multiple Coulomb scattering in the atmosphere and in the detector shielding may change the muon direction. It is evident that the reconstruction of the longitudinal

development of the muon component by means of triangulation [2, 3] provides a powerful tool for primary mass measurement [4], giving an information similar to that obtained with the Fly's Eye experiment, but in the energy range not accessible by the detection of fluorescence light. Muon tracking allows also the study of hadron interactions by means of the muon pseudorapidity [5]. Already in the past, analytical tools have been developed which describe the transformation between shower observables recorded on the ground and observables which represent directly the longitudinal shower development [7]. Fig. 1 in ref [8] shows the experimental environment. Measured core position distributions for showers inside KASCADE range from 40 - 120 m and inside Grande from 250 - 360 m. The shower core position ranges cover full trigger efficiency as confirmed by investigations of muon lateral density distributions [6]. With CR studies very high energies are accessible in the 'knee' energy region  $10^{15} - 10^{16.5}$  eV, which correspond to CM energies in the nucleon-nucleon system from 1.4 - 8 TeV currently covered by the Tevatron and the LHC. Provided, that it is feasible to focus on the first encounters with the atmospheric nuclei, muon multiplicity studies may provide insight into the high energy interaction at around 8 TeV. In this energy range saturation physics is expected to en-

\*corresponding author, e-mail: paul.doll@kit.edu

<sup>†</sup>now at: Instituto de Física y Matemáticas, Universidad Michoacana, Morelia, Mexico

<sup>2</sup> now at: Max-Planck-Institut für Physik, München, Germany

<sup>3</sup> now at: Universidade São Paulo, Instituto de Física de São Carlos, Brasil

<sup>4</sup> now at: Dept. of Astrophysics, Radboud University Nijmegen, The Netherlands

<sup>5</sup> now at: Institute for Space Sciences, Bucharest-Magurele, Romania

<sup>6</sup> deceased

<sup>7</sup> now at: University of Trondheim, Norway

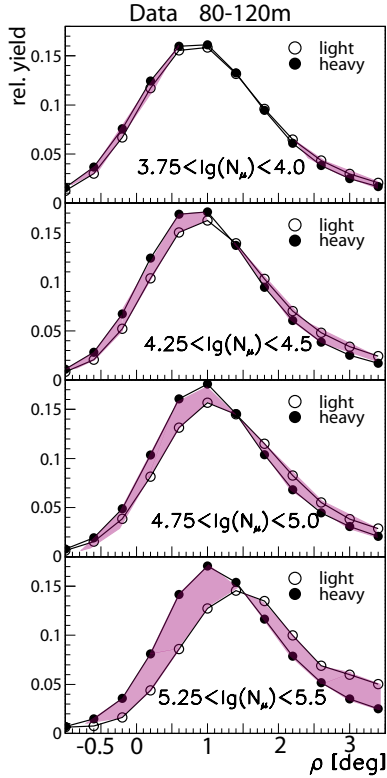


Figure 1:  $\rho$  angle distributions (normalized to integral yield equal to one) for different muon size bins and different  $\lg(N_\mu)/\lg(N_e)$  ratio above 0.83 ('heavy') and below 0.83 ('light'), for 80 - 120 m core distance range and shower direction  $\Theta = 0^\circ - 18^\circ$ . Lines connect points.

ter (rise of  $\langle p_T \rangle$ ) which is transformed to geometric scaling [14] by the color-glass-condensate theory.

## 2. Muon Production Height

The angular correlation of the muon tracks with respect to the shower axis is expressed by the  $\rho$  and the  $\tau$  angles [1]. The  $\rho$  angle contains some scattering which is represented by the  $\tau$  angle value exhibiting a  $\sigma_\tau \sim 0.2^\circ$ .

Fig. 1 shows  $\rho$  angle distributions for specific muon number  $\lg(N_\mu)$  bins corresponding to different shower energy bins [4]. The  $\rho$  angle distributions are plotted for 'light' and 'heavy' primary CR mass enriched showers, employing the  $\lg(N_\mu)/\lg(N_e)$  ratio (corrected for attenuation) [9] [4] to be larger ('heavy') or smaller ('light') than 0.83. The distributions show a dependence on the primary mass range, however, masked by the energy dependent penetration.

Based on  $\rho$  and  $\tau$  angles and the distance of the muon hit to the shower core  $R_\mu$ , the muon production height  $h_\mu$  along the shower axis is calculated:

$$h_\mu = R_\mu / \tan(\rho - |\tau|) \quad (1)$$

The MTD-KASCADE system with its dense array grid and 80 - 120 m core distance range for the muon track allows to study the muon momenta in the 100 - 200 GeV range.  $h_\mu$  will be considered for  $\rho > \tau$  which we can extend up to 20 km for a shower core muon hit distance window 80 - 120 m (note  $100 \text{ m}/20000 \text{ m} \cong 0.28^\circ$ ) employing, according to simulations,  $\sim 200 \text{ GeV}$  muons from above 15 km. Fig. 2 shows muon production height distributions for different muon size bins and different  $\lg(N_\mu)/\lg(N_e)$  ratio above 0.83 ('heavy') and below 0.83 ('light'). CORSIKA [12] simulations based on QGSjetII+FLUKA2002.4 (slope -2.7 and -3.1 below and above the knee, respectively) for Hydrogen and Iron are shown in the Fig. 2 as well. In the low  $h_\mu$  range the low energy interaction model (FLUKA2002.4) seems capable to describe the  $h_\mu$  distribution. The experimental distributions are getting more narrow with increasing energy but differently for 'light' and 'heavy' CR primaries. The  $S_{NN}$  numbers quote the CM energies assuming  $A=1$  CR primary. In the course of the analysis in [4],  $h_\mu$  is transformed to  $H_\mu$  [ $g/cm^2$ ] and after subtracting from each  $H_\mu$  an 'energy' dependent penetration depth the remaining depth  $H_\mu^A$  exhibits [4] the mass  $A$  sensitivity. Mass resolution is limited and  $\langle H_\mu^A \rangle \sim \langle H_\mu^H \rangle - 30 g/cm^2 \ln A$  [4].

Fig. 2 shows strong reduction of muons from above 15 km for 'light' primary CR particles with respect to Monte-Carlo especially for the highest energy interval, which corresponds to a CM energy of  $\sim 8 \text{ TeV}$ . Standard Monte-Carlo (see above) predicts for a nucleon-nucleon collision charged particle multiplicities  $\langle N_{ch} \rangle \sim 40 (2 \text{ TeV}) - 70 (8 \text{ TeV})$ . As a consequence, a fraction out of  $\sim 70 \times 200 \text{ GeV}$  parent pions are missing. Very recent results from LHC at 7 TeV report also [10] smaller  $\langle N_{ch} \rangle$  at midrapidity compared to QGSjetII. It would be worthwhile to study to which extent the simulated distributions in Fig. 2 above  $\sim 15 \text{ km}$  scale with the inelastic cross sections of H and Fe primary masses. At  $10^{16} \text{ eV}$  on Nitrogen  $\sigma_{inel}^H$  amounts to  $\sim 400 \text{ mb}$  and  $\sigma_{inel}^{Fe}$  is about 5 times larger. The ratio of charged particle multiplicities  $\langle N_{ch}^{Fe} \rangle / \langle N_{ch}^H \rangle$  amounts to about 12. Both factors lead to the difference between H and Fe seen in muons in Fig. 2 at high altitude. Therefore, we assume that about one tenth out of 70 pions lead to an invisible energy fraction corresponding to  $7 \times 200 \text{ GeV}$  ( $\sim 1 \text{ TeV}$ ) of the incident energy of  $\sim 10^{4.5} \text{ TeV}$ . For lower production height a regular shower development is taking over and described by the low energy interaction model FLUKA2002.4. The slower development

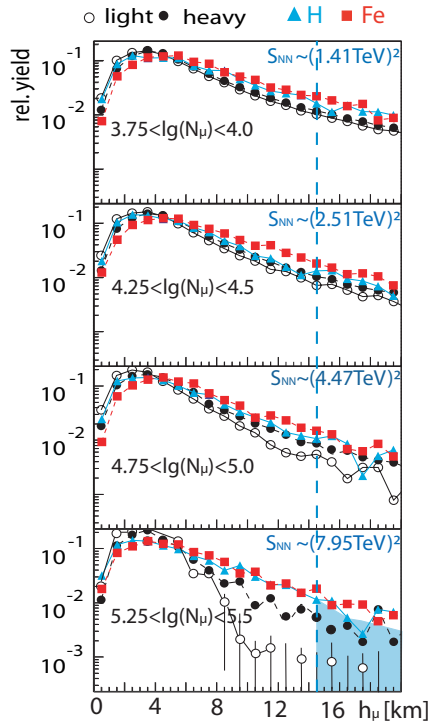


Figure 2: Muon production height distributions (normalized to integral yield equal to one) for different muon size bins and different  $\lg(N_\mu)/\lg(N_e)$  ratio above 0.83 ('heavy') and below 0.83 ('light') and 80 - 120 m core distance range and for shower direction  $\Theta = 0^\circ - 18^\circ$ . Also CORSIKA simulations based on QGSjetII + FLUKA2002.4 are given for Hydrogen (H) and Iron (Fe) CR primaries. Lines connect points.

of showers seen in the 'light' data compared to simulated H, points in a classical picture to more  $\pi$  decays in the simulations or more  $\mu$  decays in the data, however, can not be reached by decreasing  $\sigma_{inel}$  in MC in the range as discussed in [11].

The deviation from standard high energy Monte-Carlo is strongest for the 'light' CR primaries for which the quoted  $\sqrt{S_{NN}}$  is around 8 TeV. The observation that 'heavy' primaries show less deviation from the Fe prediction, points to a possible threshold effect for the 'light' CR primaries.

### 3. Muon Pseudorapidity

To investigate the deviation from the QGSjetII simulations in Fig. 2 above 15 km especially for the highest energy bin, pseudorapidity spectra for muon production height  $h_\mu$  larger than 15 km have been calculated based on the  $\rho$  and  $\tau$  angles as introduced in

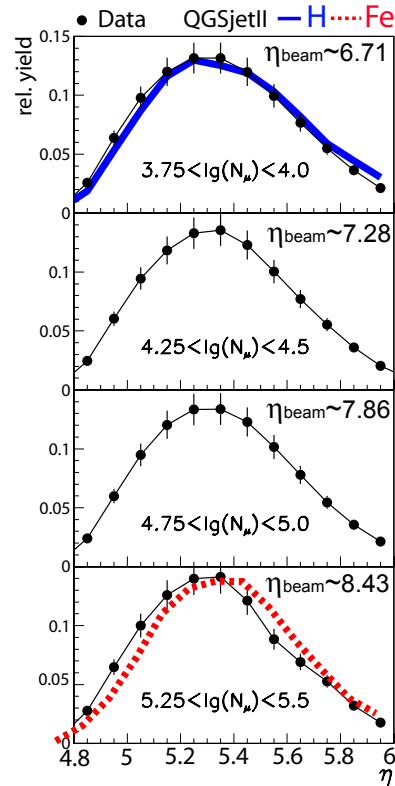


Figure 3: Pseudorapidity spectra (normalized to integral yield equal to one) for muon production height  $h_\mu$  larger than 15 km and 80 - 120 m core distance range and for shower direction  $\Theta = 0^\circ - 18^\circ$ . CORSIKA simulations based on QGSjetII + FLUKA2002.4 are given for Hydrogen (H) and Iron (Fe) CR primaries. Lines connect points.

[5].

$$\eta \simeq \ln(2p_{||}/p_T) \simeq -\ln(\sqrt{\rho^2 + \tau^2}/2) \quad (2)$$

The pseudorapidity distributions are taken in the same  $N_\mu$  size bins. The little variation of the  $\eta$  distributions is to some extent due to our analysis window (15 - 20 km). With our analysis window we filter out pions around their first interactions. Only very few 'prompt' muons will be present from the very first interaction. We have to keep in mind that after a definite number of interactions pion's probability of decay exceeds that of arriving at the next interaction level. One should note, that there is only little difference between  $\eta(\text{pion})$  and  $\eta(\text{muon})$  [5]. From independent studies with accelerators the effective beam energy for charged particle production (inelasticity  $K \simeq 0.3$ ) is quoted to be about  $0.3 \times E_0$  [13]. Effective beam rapidities  $\eta_{beam}$  are quoted in the Fig. 3 assuming  $A=1$  CR primary mass interacting in the atmosphere.

Good agreement for Hydrogen below the 'knee' and for Iron above the 'knee' is observed. Comparison of  $\eta$  distribution for 'light' CR primaries and simulated H in the highest energy bin suffers from limited statistics.

For the understanding of the  $\eta_{peak}$  positions far away from  $\eta_{beam}$  the following considerations may apply. When taking into account that the CR mass increases up to mass  $A \sim 56$ , beam rapidities are modified by  $-0.5 \ln A$ , leading to very similar  $\tilde{\eta}_{beam}$  values. While the total energy increases from  $10^{15} - 10^{16.5}$  eV we know [4] [15] (in the frame of QGSjet) that the mean mass of the CR primaries increases from  $\langle A \rangle \sim 4$  to  $\langle A \rangle \sim 56$ . Therefore, correcting the quoted  $\eta_{beam}$  gives the  $\tilde{\eta}_{beam}$  values.

However these  $\tilde{\eta}_{beam}$  values exhibit a further shift to the  $\eta_{peak}$  values possibly due to geometric scaling [14].

$$\eta_{peak} = (1/(1+\lambda)) \times (\tilde{\eta}_{beam} - \ln A^{1/6}), \quad \lambda \sim 0.2 \quad (3)$$

The  $\eta$  distributions are described by Monte-Carlo. Therefore, Monte-Carlo are able to cover the  $p_{\parallel}$  and  $p_t$  for the muons which stem mostly from charged pions. Pions are considered to dominate at midrapidity, but here we deal with the pions in the fragmentation region which deliver muons conserving the rapidity of the parent mesons. With respect to the effect of missing muons at the highest energy, representing a separate feature, the comparison with other type of high energy interaction model would be of interest. If this effect is real, it should occur again at  $\sim 10^{18}$  eV for 'heavy' CR particles.

## 4. Conclusions

Muon tracking allows to investigate  $h_{\mu}$  and  $\eta$ . Future analysis of other shower angle bins and a larger and improved quality data sample will provide a more detailed information on the nature of high energy shower muons. Also muon multiplicities provide valuable parameters to support the study of the relative contributions of different primary cosmic ray particles. A natural extension towards even larger shower energies is provided by KASCADE-Grande [16].

## Acknowledgments

The KASCADE-Grande experiment is supported by the BMBF of Germany, the MIUR and INAF of Italy, the Polish Ministry of Science and Higher Education (Grant for 2009-2011), PPP-DAAD Project for

2009-2010, and the Romanian Authority for Scientific Research CNCSIS-UEFISCSU (Grant PNII-IDEI no.461/2009 and project PN09 37 01 05).

## References

- [1] P. Doll *et al.*, Nucl.Instr.and Meth. A488 (2002) 517.
- [2] M. Ambrosio *et al.*, Nucl. Phys. (Proc.Suppl.) 75A (1999) 312.
- [3] R. Obenland *et al.*, (KASCADE Coll.), Proc. 29th ICRC, Pune, India, Vol.6 (2005) 225.
- [4] P. Doll *et al.*, (KASCADE-Grande Coll.), Nucl. Phys.B (Proc.Suppl.) 196 (2009) 114; P. Doll *et al.*, (KASCADE-Grande Coll.), Proc. 31th ICRC, Lodz, Poland, Forschungszentrum Karlsruhe Report FZKA 7516 (2009) 45; W.D. Apel *et al.*, (KASCADE-Grande Coll.), submitted to Astropart. Phys..
- [5] J. Zabierowski *et al.*, (KASCADE Coll.), Proc. 29th ICRC, Pune, India, Vol.6 (2005) 357; J. Zabierowski *et al.*, (KASCADE Coll.), Proc. 30th ICRC, Merida, Mexico, Vol.4 (2007) 111.
- [6] P. Luczak *et al.*, (KASCADE-Grande Coll.), Proc. 31th ICRC, Lodz, Poland, Forschungszentrum Karlsruhe Report FZKA 7516 (2009) 41.
- [7] L. Pentchev and P. Doll, J.Phys.G: Nucl.Part.Phys. 27 (2001) 1459.
- [8] J. Zabierowski *et al.*, (KASCADE-Grande Coll.), Nucl. Phys.B (Proc.Suppl.) 196 (2009) 114.
- [9] J.H. Weber *et al.*, (KASCADE Collaboration), Proc. 25th ICRC, Durban, South Africa Vol.6 (1997) 153
- [10] R. Engel, 16th ISVHECRI 2010, Batavia, IL, USA, <http://www.slac.stanford.edu/econf>.
- [11] R. Ulrich, 16th ISVHECRI 2010, Batavia, IL, USA, <http://www.slac.stanford.edu/econf>.
- [12] D. Heck *et al.*, Forschungszentrum Karlsruhe Report FZKA 6019, (1998); A. Fasso *et al.*, CERN-2005-10, INFN/TC-05/11, SLAC-R-773 (2005); S. Ostapchenko, Phys.Rev. D74 (2006) 014026.
- [13] J.F. Grosse-Oetringhaus and K.Reygers, J.Phys. G: Nucl. Phys. 37 (2010) 083001, E.L. Feinberg, Phys.Rep. 5 (1972) 237
- [14] Y. Mehtar-Tani and G. Wolschin, Phys.Rev. C80 (2009) 054905
- [15] T. Antoni *et al.*, (KASCADE Coll.), Astropart. Phys. 24 (2005) 1.
- [16] W.D. Apel *et al.*, (KASCADE-Grande Coll.), Nucl.Instr.and Meth. A620 (2010) 202.